

Magnitude and direction of motion with speckle correlation and the optical fractional Fourier transform

Damien P. Kelly, Bryan M. Hennelly, and John T. Sheridan

The optical fractional Fourier transform (OFRT) in combination with speckle photography has previously been used to measure the magnitude of surface tilting and translation. Previous OFRT techniques used to determine motion have not been able to discern the direction of the tilt and translation. A simple new approach involving use of correlation is presented to overcome this limitation. Controlled variation of the minimum resolution and dynamical range of measurement is demonstrated. It is then experimentally confirmed that if a rigid body's motion is captured by two OFRT systems of different orders, the direction and magnitude of both the tilting and the in-plane translation motion of the body can be independently determined without *a priori* knowledge. The experimental results confirm the validity of previous theoretical predictions. © 2005 Optical Society of America

OCIS codes: 120.6150, 070.0070, 120.3940, 070.6020.

1. Introduction

Speckle photography is a practical means of measuring in-plane translation (displacement) and tilting (rotation) motion.¹⁻⁴ Tilt, for example, can be measured by capturing the optical Fourier transform (OFT) of the reflected surface field.³ Adding or subtracting two such sequential images and numerically calculating the Fourier transform (FT) of the result produces a set of fringes whose period is inversely proportional to the constant shift in field spatial frequency, and thus the surface tilt angle can be found. A distinct disadvantage to this approach is that it does not allow the user to determine in which direction the object has been tilted. To overcome the limitation of this OFT system, we now propose to correlate the two captured sequential images, allowing both the motion direction and the magnitude to be estimated. We note that such correlation techniques have previously been used with speckle fields to discern translation motion magnitude and direction.³

The optical fractional Fourier transform (OFRT) was introduced in optics to describe wave propagation in gradient-index media; however, methods to implement the OFRT with bulk optics also exist.⁵⁻¹¹ The fractional Fourier transform (FRT) order indicates the domain into which it transforms, and an order of $\alpha = 1$ is simply the FT. The FRT angle θ is related to the FRT order by $\theta = \alpha(\pi/2)$. Several ways of applying the OFRT in speckle-based metrology systems have been proposed.¹²⁻¹⁶ However, none of these systems predict the direction of the motion. In this paper we combine the extra flexibility associated with the OFRT with a correlation-based approach and experimentally examine the resolution and detectable dynamical range of the resulting metrology system.

It has been shown theoretically¹² that it is possible to completely determine the magnitudes of both the in-plane translation and the tilting motion of a rigid body, if this motion is captured simultaneously in two different fractional Fourier domains [$a_1(\theta_1)$ and $a_2(\theta_2)$]. With the correlation technique it is now possible to build up a much more complete picture of the motion of a rigid body, without *a priori* knowledge. Experimental results are presented confirming the validity of the theory. The experimental setup was demonstrated to be capable of measuring translation motion over the range $10 < x < 1000 \mu\text{m}$ and tilting motion over the range $0.0005 < \alpha < 0.0087$ rad between individually captured frames. The system, as demonstrated, is both flexible and was implemented for a cost of approximately \$10,000.

The authors are with the Department of Electronic and Electrical Engineering, Faculty of Architecture and Engineering, University College Dublin, Belfield, Dublin 4, Republic of Ireland. J. T. Sheridan's e-mail address is john.sheridan@ucd.ie.

Received 30 August 2004; revised manuscript received 23 December 2004; accepted 15 January 2005.

0003-6935/05/142720-08\$15.00/0

© 2005 Optical Society of America

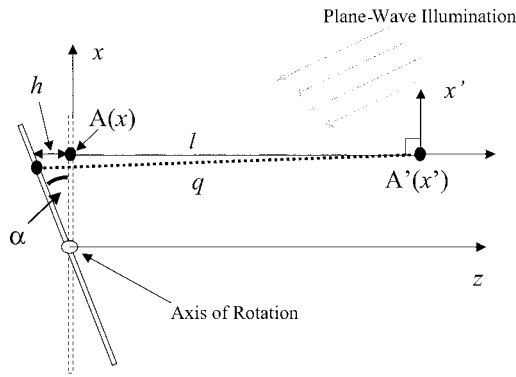


Fig. 1. Relating the tilt angle α to the reflected speckle field.

2. Optical Fractional Fourier Transform–Based Correlation Technique

It is necessary to clearly determine how the reflected speckle field before rotation $u(x)$ is related to the speckle field after rotation (tilt). In Fig. 1 the rigid body before rotation is depicted as the dashed rectangle and after rotation as a solid rectangle. Let us consider how light reflected from point $A(x)$ in Fig. 1 effects point $A'(x')$. Let $x = x'$, so that the distance between the two points is l , which is perpendicular to both the x and x' axes. Before rotation the incident plane wave strikes $A(x)$ and is reflected along the z axis, a distance l , where it contributes to the intensity and phase of the point $A'(x')$. After rotation, the plane wave again strikes $A(x)$. This time, however, the plane wave must travel an extra distance approximately equal to h to reach the same point $A(x)$. If this plane wave contributes to the point $A'(x')$, it must be reflected along the dotted line q . However, if α is small it follows that $h \ll l$ and that also $q \approx l + h$. So the plane wave after rotation will have to travel a total further distance approximately equal to $2h$. A plane wave can be described as $\exp(j2\pi z/\lambda)$ where λ is the wavelength and z is the distance along the axis. Thus, after traveling a further distance $2h$, the extra phase accumulated is given by $\exp(j4\pi h/\lambda)$. It can be shown that if the angle α is small, $h = x \sin(\alpha) \approx x\alpha$. Thus the reflected speckle field $u(x)$ after rotation can be approximated by $u(x)\exp[j(2\pi/\lambda)\kappa x]$, where $\kappa \approx 2\alpha$.

The rotation of a rigid body can be determined by an OFT system.⁴ Once again let the reflected speckle field from an object before rotation be described by $u(x)$. After it is tilted it becomes as $u(x)\exp[\pm j(2\pi/\lambda)\kappa x]$ where the sign depends on the direction of the rotation. The reflected speckle field is passed through a bulk optical system, which performs an OFT on the field. Thus the field captured by the camera is the intensity of the FT of the original reflected speckle field, which before tilting is given by $\tilde{I}(k) = |\text{FT}\{u(x)\}|^2(k)$ and after tilting by $\tilde{I}(k \mp f\kappa)$, where f is the focal length of the lens used in the optical system. Correlating these two images gives

$$\text{Corr}(k) = \tilde{I}(k \mp f\kappa) \otimes \tilde{I}(k). \quad (1)$$

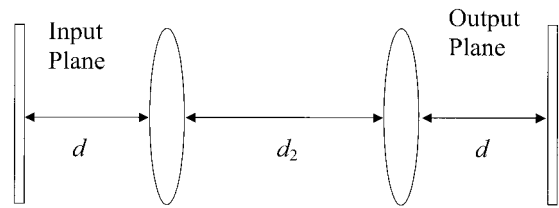


Fig. 2. Bulk optical system for implementing OFRT.¹¹

For simplicity let us assume at first that the intensities $\tilde{I}(k)$ and $\tilde{I}(k \mp f\kappa)$ are identical apart from the shift of $\mp f\kappa$. The function $\text{Corr}(k)$ will have a peak when the images $\tilde{I}(k)$ and $\tilde{I}(k \mp f\kappa)$ overlap, which occurs when $k = \mp f\kappa$. Thus, if the peak occurs when $k = +f\kappa$, the object has been tilted in the negative direction whereas if the peak occurs when $k = -f\kappa$ the object has been tilted in the positive direction. It should be noted that the detectable resolution and dynamical range are fixed and depend on the reflected speckle field size (roughness of the surface) and the sensitivity of the measurement system, e.g., numerical aperture, camera area, and pixel size.

Now let us consider the situation in which the reflected speckle field from an object is passed through an OFRT system. The reflected speckle field from an object after it is tilted is again modeled as $u(x)\exp(\pm j\kappa x 2\pi/\lambda)$. However, this time the reflected speckle field is passed through the bulk optical system shown in Fig. 2 and described by Cai and Wang.¹¹ The fractional order α (fractional angle θ) and the distances d and d_2 are given by

$$\alpha = \theta \left(\frac{2}{\pi} \right) = \left(\frac{2}{\pi} \right) \arccos \left[\frac{-d(2f-d)}{(f-d)^2 + f^2} \right], \quad (2a)$$

$$d_2 = 2f \frac{d(d-f) + f^2}{(f-d)^2 + f^2}, \quad (2b)$$

where f is the focal distance of both lenses. The reader should not confuse the OFRT angle θ with the physical angle α through which the rigid body rotates.

Using the two-dimensional optical definition of the FRT of angle θ , we can give the intensity information captured at the output of the OFRT system by

$$|F_\theta\{u(x)\}|^2(k) = \frac{1}{[\lambda f |\sin(\theta)|]^{1/2}} \left| \int_{-\infty}^{\infty} u(x) \times \exp \left[\frac{j\pi}{\lambda f} x^2 \cot(\theta) - \frac{2j\pi x k}{\lambda f} \csc(\theta) \right] dx \right|^2. \quad (3)$$

Following tilting the image (OFRT) plane intensity is given by

$$\begin{aligned} \tilde{I}_0(k) &= \left| F_0\{u(x)\} \exp\left(\pm j \frac{2\pi}{\lambda} \kappa x\right) \right|^2 (k) \\ &= \frac{1}{|\lambda f \sin(\theta)|^{1/2}} \left| \int_{-\infty}^{\infty} u(x) \exp \right. \\ &\quad \times \left. \left(\pm j \frac{2\pi}{\lambda} \kappa x \right) \exp \left[\frac{j\pi}{\lambda f} x^2 \cot(\theta) \right. \right. \\ &\quad \left. \left. - \frac{2j\pi x k}{\lambda f} \csc(\theta) \right] dx \right|^2. \end{aligned} \quad (4)$$

This integral can be rewritten as

$$\begin{aligned} \tilde{I}_0[k \mp \kappa f \sin(\theta)] &= |F_0\{u(x)\}|^2 [k \mp \sin(\theta) f \kappa] \\ &= \frac{1}{|\lambda f \sin(\theta)|^{1/2}} \left| \int_{-\infty}^{\infty} u(x) \exp \left\{ \frac{j\pi}{\lambda f} x^2 \right. \right. \\ &\quad \times \cot(\theta) - \frac{j2\pi x}{\lambda f} \csc(\theta) \\ &\quad \left. \left. \times [k \mp \sin(\theta) f \kappa] \right\} dx \right|^2. \end{aligned} \quad (5)$$

Comparing this with Eq. (3) we can see that the fractional domain parameter has been shifted by an amount $\kappa f \sin(\theta)$. Correlating the two images corresponds to

$$\text{Corr}(k) = \tilde{I}[k \mp \kappa f \sin(\theta)] \otimes \tilde{I}(k). \quad (6)$$

The direction and size of the tilting can be determined in the same manner as outlined above. The magnitude of the shift in the fractional domain k is now given by $\mp \kappa f \sin(\theta)$. Furthermore it should be clear that by changing θ , the fractional order, the resolution and dynamical range associated with the metrology system can also be varied. This result is discussed further and confirmed experimentally in Section 3.

We want to simultaneously measure tilt and in-plane translation motion using two fractional orders. To do so, we assume that two OFRT systems are available, system 1 and system 2 (see the schematic diagram in Fig. 3) corresponding to two different fractional angles θ_1 and θ_2 (corresponding to orders a_1 and a_2 , respectively).¹¹ After the field passes through optical system 1, the field incident on camera 1 is given by

$$\begin{aligned} \tilde{I}_{\theta_1}(k) &= |F_{\theta_1}\{u(x)\}|^2(k) \\ &= \frac{1}{|\lambda f \sin(\theta_1)|^{1/2}} \left| \int_{-\infty}^{\infty} u(x) \exp \left[\frac{j\pi}{\lambda f} x^2 \cot(\theta_1) \right. \right. \\ &\quad \left. \left. - \frac{2j\pi x k}{\lambda f} \csc(\theta_1) \right] dx \right|^2. \end{aligned} \quad (7)$$

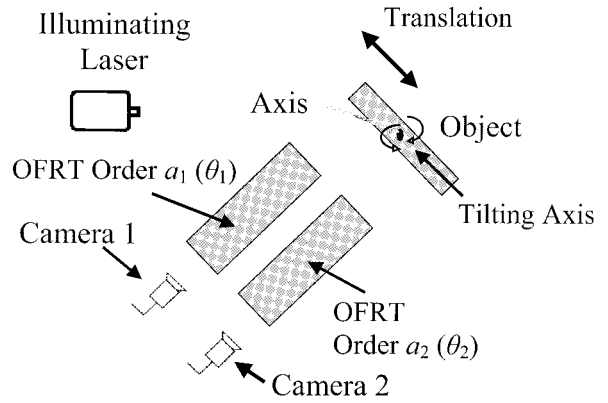


Fig. 3. Optical arrangement used to determine tilt and in-plane translation motion.

The object is now translated by an amount ζ and tilted by an amount κ . The reflected field can now be described as $u(x \pm \zeta) \exp[\pm j(2\pi/\lambda)\kappa x]$ and the OFRT is given by

$$\begin{aligned} \tilde{I}_{\theta_1}\{k \mp [\zeta \cos(\theta_1) + \kappa f \sin(\theta_1)]\} \\ &= \left| F_{\theta_1} \left[u(x \pm \zeta) \exp \left(\pm j \frac{2\pi}{\lambda} \kappa x \right) \right] \right|^2 (k) \\ &= \frac{1}{|\lambda f \sin(\theta_1)|^{1/2}} \left| \int_{-\infty}^{\infty} u(x) \exp \left[\frac{j\pi}{\lambda f} x^2 \cot(\theta_1) \right. \right. \\ &\quad \left. \left. - \frac{j2\pi x}{\lambda f} \csc(\theta_1) (k \mp Q_1) \right] dx \right|^2, \end{aligned} \quad (8)$$

where $Q_1 = \zeta \cos(\theta_1) + \kappa f \sin(\theta_1)$.

Comparing Eqs. (7) and (8) we can see that the fractional domain parameter k has been shifted by an amount $Q_1 = \zeta \cos(\theta_1) + \kappa f \sin(\theta_1)$. Correlating the two images yields

$$\text{Corr}(k) = \tilde{I}(k \mp Q_1) \otimes \tilde{I}(k), \quad (9)$$

from which we can determine a value for Q_1 . A similar analysis is carried out for system 2, and a value for $Q_2 = \zeta \cos(\theta_2) + \kappa f \sin(\theta_2)$ can be measured. Geometrically we have projected the same motion onto two nonorthogonal axes.¹⁴ We note that we now have two simultaneous equations with unknowns κ and ζ , which can be solved to yield

$$\zeta = \csc(\theta_1 - \theta_2) [Q_2 \sin(\theta_1) - Q_1 \sin(\theta_2)], \quad (10a)$$

$$\kappa = \csc(\theta_1 - \theta_2) [Q_1 \cos(\theta_2) - Q_2 \cos(\theta_1)] / f. \quad (10b)$$

Recalling that $\kappa \approx 2\alpha$, Eq. (10b) can be written as

$$\alpha \approx \csc(\theta_1 - \theta_2) [Q_1 \cos(\theta_2) - Q_2 \cos(\theta_1)] / 2f. \quad (10c)$$

It is desirable at this point to define explicitly what we mean by the term system range. For correlation to occur there must be an imaged surface area of speckle, i.e., a part of the field, that is common to both captured images. The area common to both images will decrease as the body is moved. In the extreme case there will be no area of speckle common to both images, total decorrelation will occur, and it will not be possible to measure any motion. The point at which a correlation peak can no longer be unambiguously identified can be used to define the absolute limiting range of the metrology system, i.e., the largest motion measurable.

Examination of Eq. (6) reveals that if a body is tilted by an amount κ , the relevant fractional domain parameter is shifted by an amount $\kappa f \sin(a\pi/2)$. Thus, if a is large ($0.7 < a < 1$), then $\sin(a\pi/2)$ is closer to unity and the fractional parameter is more sensitive to changes in κ (it can be used to measure fine rotations). However, this also means that the range of the system will be reduced because a small motion of the rigid body results in a large motion in the output plane of the system, reducing the amount of speckle common to both images and thus reducing the correlation between the images. If, on the other hand, one wishes to measure a large tilting motion, a lower order ($0.1 < a < 0.5$) is more suitable. By choosing a lower value of a one has to rotate the rigid body through a larger angle to achieve the same shift in the fractional domain. Thus the range of the system has been increased but the sensitivity has been reduced.

Similarly, when we are measuring translation it can be shown that if a body is translated by ζ , the relevant fractional domain parameter is shifted by an amount $\zeta \cos(a\pi/2)$. Thus if a is small (close to zero) then $\cos(a\pi/2)$ is close to unity and the fractional parameter is more sensitive to ζ variations. Conversely, for a low fractional order, i.e., $0.1 < a < 0.5$, translational motion can be measured more sensitively; however, the range of the system is reduced.

Therefore there is a trade-off when we are choosing a fractional order between being able to measure a very small motion accurately over a small range or being able to measure less accurately but over a larger range. This trade-off depends on whether tilt or translation are of primary concern and should be borne in mind when one is deciding what fractional order would be most suitable for a given application. For example, to produce a metrology system that is able to measure large translational motion, or a small rotational motion, a high fractional order ($a = 0.7$) would be most suitable.

3. Experimental Results

We now discuss the implementation of the OFRT-based correlation system.

A. Experimental Setup

The rigid body in this experiment is an optically rough 1.5 cm by 1.5 cm square piece of metal. It was

illuminated at an angle of 35° by a collimated plane wave from a 488-nm argon laser. The focal length f of the lenses used was 10 cm. Since the lengths in the system could only be imperfectly positioned with an accuracy of approximately ± 1 mm, it was estimated that a FRT angle θ implementation accuracy of approximately $\pm 1.2^\circ$ could be achieved (see Section 4). It must also be noted that positioning errors also lead to variations in system magnification. In an attempt to ensure consistency, averaging of the tilt results was carried out over many independent measurements. The camera used was a Sony XC-ES50CE, and the translation and rotation stages were driven with Oriel Encoder Mike actuators controlled with the 18113 Oriel Encoder Mike Control System. From the technical specifications for the Oriel Encoder Mike, driving the rotation stage a distance of $161 \mu\text{m}$ causes a rotation of 1° or 0.0174 rads. Both motion stages (rotation and translation) are rated to have a position resolution of $0.1 \mu\text{m}$. However, we found that, because of the weight of the rig (including the rigid body), the increased hysteresis, and the dead-zone effects (see Section 4), only a motion of $\sim 5 \mu\text{m}$ could be reliably achieved. National Instruments LabVIEW was used to grab and process the captured images.

B. Determining the Tilting Direction

An OFT system $a = 1.0$ ($\theta = \pi/2$, $d = 200$ mm, $d_2 = 300$ mm) was implemented. The first image was grabbed, and then the rotational stage was turned through an angle α . Then a second image was grabbed. Processing (correlating) produced the result shown in Fig. 4(a). The correlation peak in the center results from the normalized (with respect to the maximum autocorrelation peak size) autocorrelation of the first image. It thus has the maximum value of unity and its position indicates the origin, i.e., the initial location of the plate.

The second correlation peak is the normalized correlation of the first and second images. It is in a different location (to the right of the origin indicating that motion in a particular direction has occurred), and the height of the peak is less than unity, which means that the images are not identical, i.e., some decorrelation has occurred. By determining the difference between the location of the first (origin) and second peaks, we can determine the angle through which the body has been rotated. The rigid body was rotated through an angle of $\alpha = 0.00055$ rad (0.032°) and the angle measured was 0.00047 (0.027°).

The decreasing height of the second correlation peak determines the maximum measured amount the body can be rotated through. In the extreme case, the rigid body is rotated through such a large angle that total decorrelation between the two images occurs. In this case there will be no measurable second correlation peak, and the amount of rotation can no longer be determined. In this paper a correlation peak of less than 0.2 is considered to be the limiting range of the system. It should be noted that this

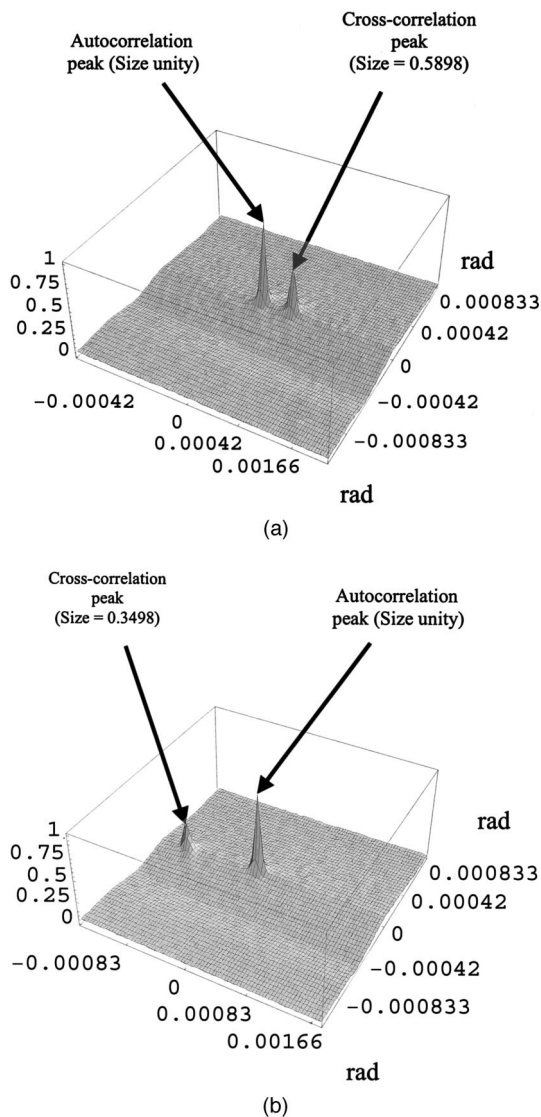


Fig. 4. (a) Clockwise rotation of angle $\alpha = 0.0005$ rad in an OFRT system of order $a = 1$ (OFT). (b) Anticlockwise rotation of angle $\alpha = 0.0011$ rad in an OFRT system of order $a = 1$ (OFT).

choice was imposed by us only for reasons of simplicity and that no postprocessing of the data to improve the signal-to-noise ratio was carried out.

The rotational stage was then returned to its original position. Again a first image was grabbed, and the rotational stage was turned through an angle of -2α [see Fig. 4(b)] and a second image was grabbed. The images were processed in the same manner as above. It is clear that the correlation peak is now to the left of the origin. It is also twice as far from the origin as in the previous case indicating that the body has been rotated through an angle twice the size and in the opposite direction. The height of the correlation peak is also less than in Fig. 4(a) indicating that the correlation between the two images decreases as the body is rotated through larger angles. In this case the rigid body was rotated through an

angle of $-2\alpha = 0.0011$ rad (0.063°) and the angle measured was 0.0011 rad (0.063°).

C. Varying the Dynamical Range of the Metrology System

1. Tilting Measurement

An OFRT system of fractional order of $a = 1.2$ ($d = 172.6$ mm, $d_2 = 295.1$ mm) was implemented. The theoretical analysis indicates that the metrology system will now have a larger dynamical range for measuring tilting angles; however, it will not be able to measure tilting motion as sensitively. In Figs. 5(a) and 5(b) positive tilting of the rigid body through an angle of $\alpha = 0.0011$ rad (0.063°) was captured for orders $a = 1.2$ and 1.6 ($d = 132.5$ mm, $d_2 = 258.8$ mm). The angle α [$\alpha = 0.0011$ rad (0.063°)] through which the body was turned was measured accurately [$\alpha = 0.0011$ rad (measured value)] for both orders. It can be seen that the correlation peak in Fig. 5(a) is farther from the origin than in Fig. 5(b) (even though the rigid body has been turned through the same angle) indicating that the OFRT of order $a = 1.6$ measures the tilting angle less sensitively than an OFRT order of $a = 1.2$. However, it also means that larger angles between captured frames can be measured. Using the chosen correlation peak threshold of 0.2 as the limiting range of the metrology system, the largest angle that we can determine with an OFRT of order $a = 1.2$ is 0.0027 rad (0.154°). The largest angle that can be determined for OFRT order $a = 1.6$ is 0.0087 rad (0.498°). This represents a threefold increase in the range but is accompanied by a threefold decrease in the minimum angle measurable, i.e., a corresponding loss in sensitivity.

2. Translation Measurement

For an OFRT system the distance of the second correlation peak from the origin is given by $Q = \zeta \cos(\theta) + \kappa \sin(\theta)$. It follows that for an OFRT system of order $a = 1$ ($\theta = \pi/2$, $d = 200$ mm, $d_2 = 300$ mm, an OFT system), it is not possible to measure translation motion ζ because the ζ term is multiplied by $\cos(\theta = \pi/2)$. However, for an OFRT systems of orders $a = 1.4$ ($d = 150.9$ mm, $d_2 = 280.9$ mm) and for $a = 1.6$ ($d = 132.5$ mm, $d_2 = 258.7$ mm), translation motion can be measured with different sensitivities over different ranges. This can be seen in Figs. 5(c) and 5(d). In Figs. 5(c) and 5(d) the body is translated at a distance of $150 \mu\text{m}$; however, it is plain that for the order $a = 1.6$ the correlation peak is farther from the origin that it is for the order $a = 1.4$.

Measurements of translations of sizes 300 and $150 \mu\text{m}$ were made for OFRT systems of different fractional orders. For a system of order $a = 1.4$, the body was translated by $300 \mu\text{m}$ but the actual motion measured was $283 \mu\text{m}$ representing an error of $\sim 5\%$. The rigid body was then moved by $150 \mu\text{m}$; however, the measured motion was only $141 \mu\text{m}$ representing an error of $\sim 6\%$.

When the order is changed to $a = 1.6$, an improve-

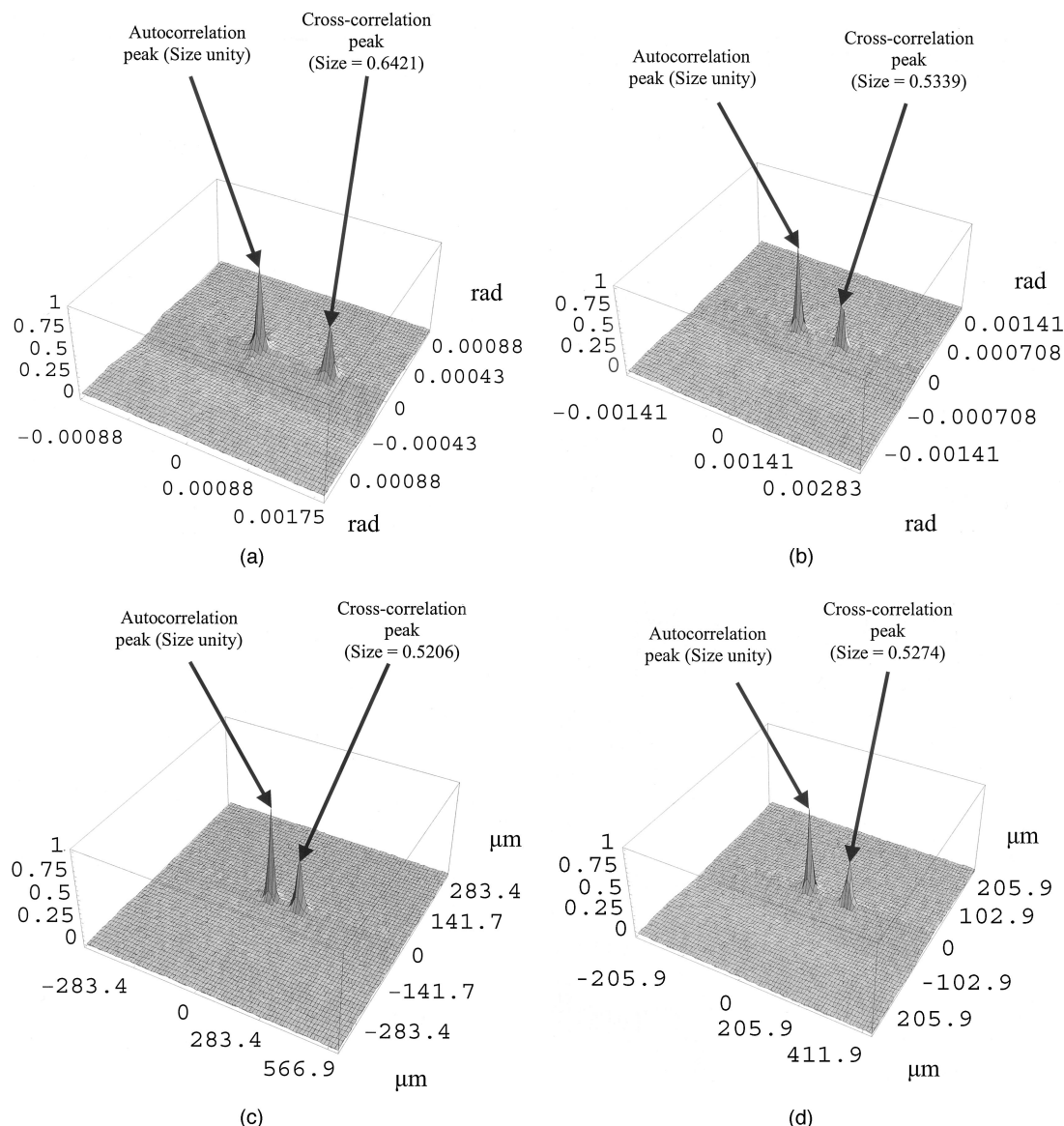


Fig. 5. (a) Clockwise rotation of angle $\alpha = 0.0011$ rad in an OFRT system of order $a = 1.2$. (b) Clockwise rotation of angle $\alpha = 0.0011$ rad in an OFRT system of order $a = 1.6$. (c) Positive translation of $150 \mu\text{m}$ in an OFRT system of order $a = 1.4$. (d) Positive translation of $150 \mu\text{m}$ in an OFRT system of order $a = 1.6$.

ment in the accuracy of the measurement was observed. The rigid body was translated again by $300 \mu\text{m}$; however, the measured result was $298 \mu\text{m}$ representing an error of $\sim 1\%$. When the rigid body was translated by $150 \mu\text{m}$, the measured result was $145 \mu\text{m}$ representing an error of $\sim 3\%$.

When the order is changed to $a = 1.8$, a further improvement in the accuracy of the measurement was noted. The rigid body was translated again by $300 \mu\text{m}$, and the measured result was $298 \mu\text{m}$ representing an error of $\sim 1\%$. When the rigid body was translated by $150 \mu\text{m}$, the measured result was $149 \mu\text{m}$ representing an error of $\sim 1\%$.

Therefore, as the fractional order is changed from $a = 1.4$ to $a = 1.8$, an improvement of the system ability to measure smaller motions more accurately is thus noted.

D. Simultaneous Tilting and Translation Measurement

To determine both tilting and translational motion it is necessary to have two simultaneous equations [see Eqs. 10(a)–10(c)]. This can be achieved as described in Section 2 by capturing the motion of the rigid body in two different fractional domains. In Fig. 6(a) the speckle fields corresponding to a translational motion of $150 \mu\text{m}$ followed by a rotation of 0.0011 rad (0.063°) were captured and processed after having passed through an OFRT system of order $a_1 = 1.4$. The same motion was also captured in an OFRT system of order $a_2 = 1.6$. Following the analysis it was found that the tilting motion was estimated to be 0.0011 rad (0.063°) and the translational motion was estimated to be $147 \mu\text{m}$. It is clear from Fig. 6(a) that the location of the cross-

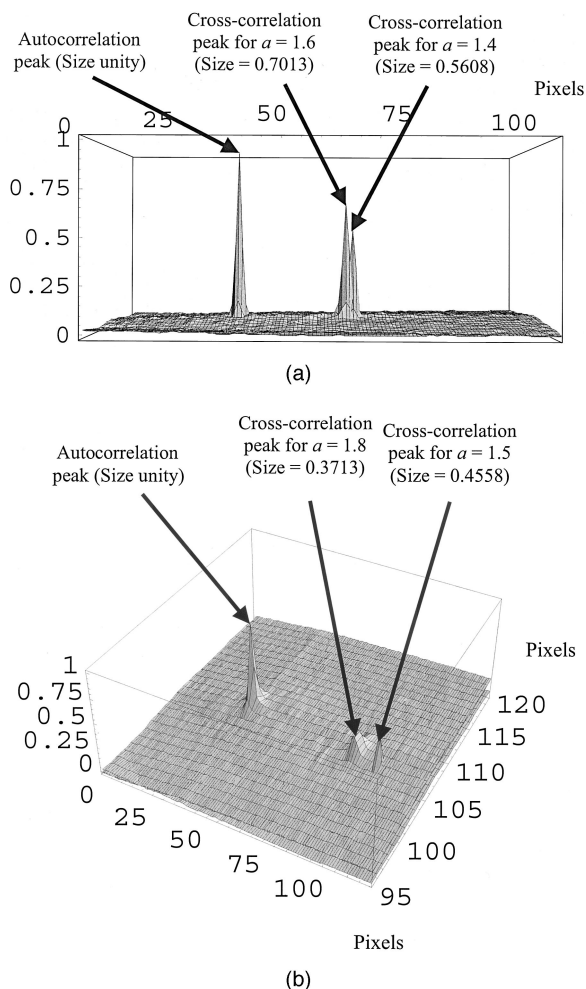


Fig. 6. (a) Positive translation of $150\ \mu\text{m}$ followed by a positive rotation of $0.0011\ \text{rad}$ for OFRT systems of order $a = 1.4$ and $a = 1.6$. (b) Positive translation of $300\ \mu\text{m}$ followed by a positive rotation of $0.0022\ \text{rad}$ for OFRT systems of order $a = 1.5$ and $a = 1.8$.

correlation peaks for orders $a_1 = 1.4$ and $a_2 = 1.6$ are very close. In fact Fig. 6(a) has purposely been plotted from a different viewpoint to allow the reader to distinguish the two cross-correlation peaks more easily.

We repeated the experiment for a translation motion of $300\ \mu\text{m}$ followed by a rotation of $0.0022\ \text{rad}$ (0.126°) using fractional orders of $a = 1.5$ ($d = 141.4\ \text{mm}$, $d_2 = 270.7\ \text{mm}$) and $a = 1.8$ ($d = 115.6\ \text{mm}$, $d_2 = 230.9\ \text{mm}$). The tilting and translational motion was found to be $0.0021\ \text{rad}$ (0.120°) and $317\ \mu\text{m}$, respectively. From Fig. 6(b) it can be seen that the resulting cross-correlation peaks are further apart than in Fig. 6(a).

4. Conclusion

We have presented an optical signal processing-based technique to determine the direction and magnitude of a rigid body's motion using correlation. An optical fractional Fourier transform (OFRT) system is proposed in which the dynamical range and sensitivity of the system can be varied as the user desires.

This new system can be used to simultaneously estimate both the tiling and the in-plane translation of a rigid body. Results have been presented illustrating the validity of the models and the effectiveness of the technique. The experimental results demonstrate the sensitivity, range, and accuracy with which tilting and translation motions can be measured.

There are several potential sources of experimental error in the data produced in the metrology system.

(1) Imperfectly positioned lenses. An error analysis was carried out to estimate the effect of imperfectly positioned lenses on the output from the OFRT. The analysis indicated that the effect of imperfectly positioned lenses ($\pm 1\ \text{mm}$) was dependent on the fractional order of the optical system. OFRT orders became increasingly sensitive to error as a is decreased from $a = 1.8$ ($d = 115.6\ \text{mm}$, $d_2 = 230.9\ \text{mm}$) (error $\sim 0.8^\circ$) to $a = 1.0$ ($d = 200\ \text{mm}$, $d_2 = 300\ \text{mm}$) (error $\sim 1.2^\circ$). It should also be noted that misalignment of optical elements will also lead to changes in the system magnification that can adversely effect the measurements. We note from our results (Subsection 3.B.2) that, with an order $a = 1.4$, translation motion was not measured as accurately as it was for an order of $a = 1.8$.

(2) Motion stages: hysteresis, integrator windup, and dead zone. The Oriel Motor positioning controller system is a standard proportional, integral, derivative controller. When attempting to move the actuator a small distance ($\sim 1\text{--}5\ \mu\text{m}$), the effects of the dead zone and integrator windup, which typically cause the motor to overshoot its position before repositioning, were observed. We found that the rig (including rigid body) was slightly too heavy for the positioning actuators and so they were not able to perform to the standard of the listed specifications. This effect is more pronounced when the distance to be moved is small. There are some hysteresis effects associated with the motor that also lead to an imprecision in positioning.

From the experimental results it appears that translational motion cannot be measured accurately (error $\pm 6\%$) for low fractional orders. This is not inconsistent with the theory allowing for the positional errors above; however, it does seem that rotational measurements can be measured more accurately over a wider range of OFRT orders. It was also noted during the course of these experiments that the accuracy of rotational measurements (even for higher fractional orders, i.e., $a > 1.5$) could be reproduced more consistently than those of the translational motion.

Our model predicted that if motion is captured simultaneously in two different fractional Fourier domains, a complete picture of the motion of a rigid body can be determined. Two results (Fig. 6) are presented here that prove that this is possible. However, two points should be noted based on our experimental results:

(1) Our initial results seem to indicate that it is

more difficult to measure translation motion accurately (particularly for $a < 1.4$), so it would seem sensible that fractional Fourier orders of $a > 1.5$ be used for any metrology system that needs to measure both tilting and translation with high accuracy.

(2) When applying this technique one should not use two fractional orders that are close to each other [see Fig. 6(a)]. Motion captured with an OFRT system causes a shift in the relevant fractional domain parameter. If these fractional orders are close to each other they will produce very similar shifts in their respective fractional domain parameters. In Fig. 6(b) one can see that, although the translation and rotation motions are larger than in Fig. 6(a), the correlation peaks are further apart, due in part to the larger difference between the fractional orders ($a = 1.5$ and $a = 1.8$) used.

We acknowledge the support of Enterprise Ireland and Science Foundation of Ireland through the Research Innovation Fund and the Basic Research Programme. We also acknowledge the support of the Irish Research Council for Science, Engineering and Technology.

References

1. P. K. Rastogi, *Digital Speckle Pattern Interferometry and Related Techniques* (Wiley, Chichester, UK, 2001).
2. W. Steinchen and L. Yang, *Digital Shearography: Theory and Application of Digital Speckle Pattern Shearing Interferometry*, Vol. 100 of SPIE Press Monographs (SPIE, Bellingham, Wash., 2003).
3. P. K. Rastogi, "Techniques of displacement and deformation measurement in speckle metrology," in *Speckle Metrology*, R. S. Sirohi, ed. (Marcel Dekker, New York, 1993), pp. 50–58.
4. H. Tiziani, "A study of the use of laser speckle to measure small tilts of optically rough surfaces accurately," *Opt. Commun.* **5**, 271–274 (1972).
5. D. Mendlovic and H. M. Ozatkas, "Fractional Fourier transformations and their optical implementations I," *J. Opt. Soc. Am. A* **10**, 1875–1881 (1993).
6. D. Mendlovic and H. M. Ozatkas, "Fractional Fourier transformation and their optical implementations II," *J. Opt. Soc. Am. A* **10**, 2522–2531 (1993).
7. A. W. Lohmann, "Image rotation, Wigner rotation, and the fractional Fourier transformation," *J. Opt. Soc. Am. A* **10**, 2181–2186 (1993).
8. R. G. Dorsch, "Fractional Fourier transform of variable order based on a modular lens system," *Appl. Opt.* **34**, 6016–6020 (1995).
9. S. Abe and J. T. Sheridan, "An optical implementation for the estimation of the fractional-Fourier order," *Opt. Commun.* **137**, 214–218 (1997).
10. A. W. Lohmann, "A fake zoom lens for fractional Fourier experiments," *Opt. Commun.* **115**, 427–443 (1995).
11. L. Z. Cai and Y. Q. Wang, "Optical implementation of scale invariant fractional Fourier transform of continuously variable orders with a two-lens system," *Opt. Commun.* **34**, 249–252 (2002).
12. J. T. Sheridan and R. Patten, "Fractional Fourier speckle photography: motion detection and the optical fractional Fourier transformation," *Optik (Stuttgart)* **111**, 329–331 (2000).
13. J. T. Sheridan and R. Patten, "Holographic interferometry and the fractional Fourier transformation," *Opt. Lett.* **25**, 448–450 (2000).
14. J. T. Sheridan, B. M. Hennelly, and D. Kelly, "Motion detection, the Wigner distribution function, and the optical fractional Fourier transform," *Opt. Lett.* **28**, 884–886 (2003).
15. D. P. Kelly, B. M. Hennelly, and J. T. Sheridan, "Speckle correlation and the fractional Fourier transform," in *Optical Information Systems II*, B. Javidi, ed., Proc. SPIE **5557**, 225–266 (2004).
16. B. M. Hennelly, D. Kelly, and J. T. Sheridan, "Wavelength-controlled variable-order optical fractional Fourier transform," *Opt. Lett.* **29**, 427–429 (2004).